AIAA 91–0825

Simulation of an Aerospace Vehicle Pitch-Over Maneuver

William L. Kleb
NASA Langley Research Center, Hampton, VA 23681
A. N. Author and Y. F. Anotherlongername
Someother Affliation, Atown, ST 98293

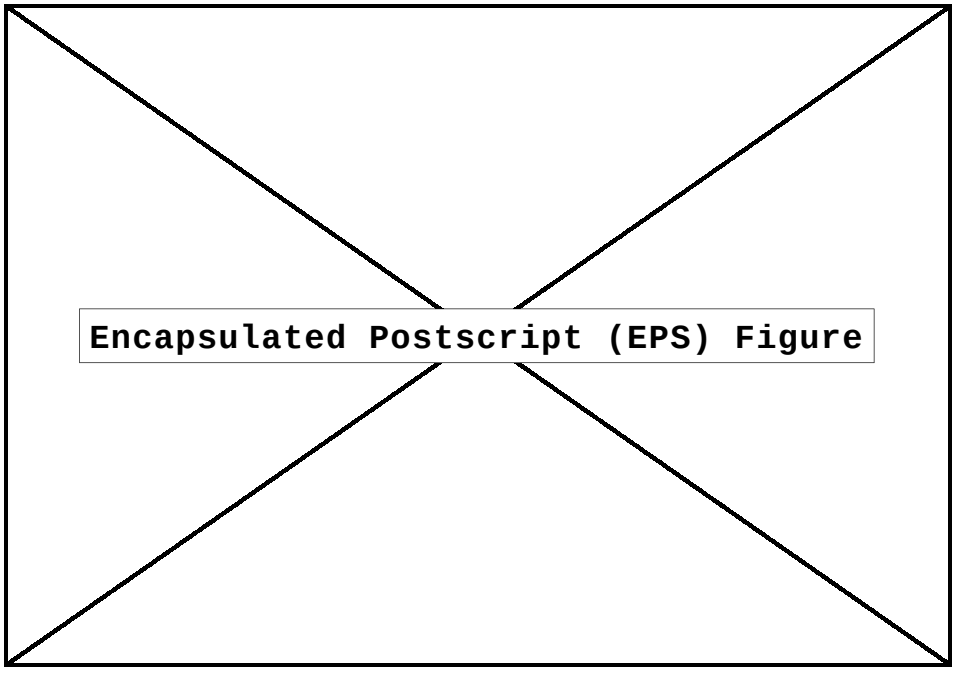

Simulation of an Aerospace Vehicle Pitch-Over Maneuver

William L. Kleb*
NASA Langley Research Center, Hampton, VA 23681

A. N. Author† and Y. F. Anotherlongername†
Someother Affliation, Atown, ST 98293

Note: this abstract does not appear when a journal note simulation is the chosen option. **The objective of the present work is to summarize the application of unsteady computational fluid dynamic methods to the problem of predicting verticle take-off/vertical landing vehicle aerodynamics during an un-powered pitch-over maneuver. In addition to the time-dependent simulation of a pitch-over maneuver, a series of steady solutions at discrete points are also computed for comparison with wind-tunnel measurements and as a means of quantifying unsteady effects. As this application represents a new challenge to unsteady computational fluid dynamics, observations concerning grid resolution, far-field boundary placement, temporal resolution, and the suitability of assuming flow-field symmetry are discussed.**

Nomenclature

c	Sound speed, m/s
M	Mach number
P	Pressure, Pa
Re_s	Reynolds number based on length s
T	Temperature, K
V	Velocity, m/s
x, y, z	Cartesian body axes, m
α	Angle of attack, deg
η	Wall-normal distance, m
ρ	Density, kg/m^3

Subscripts

tran	Transition
w	Wall
∞	Freestream

Superscripts

0	Fiduciary point
$n+1$	Time level

Introduction

NASA'S Access to Space Study[1] recommends the development of a *fully* reusable launch vehicle[2] to replace the aged Space Shuttle. *The* `\dropword` *command created the hanging capital letter and automatically capitalizes the rest of the word.* A method of reaching this goal is to develop a vehicle which does not rely on expendable boosters to reach orbit, a single-stage-to-orbit vehicle.[3] One such configuration being investigated is a Vertical Take-off and Vertical Landing (VTVL) concept.[3] In one scenario, the VTVL vehicle, upon completion of its mission in low-Earth orbit, reenters nose first, decelerates to subsonic speeds, and then performs a rotation maneuver[4–6] to land vertically.

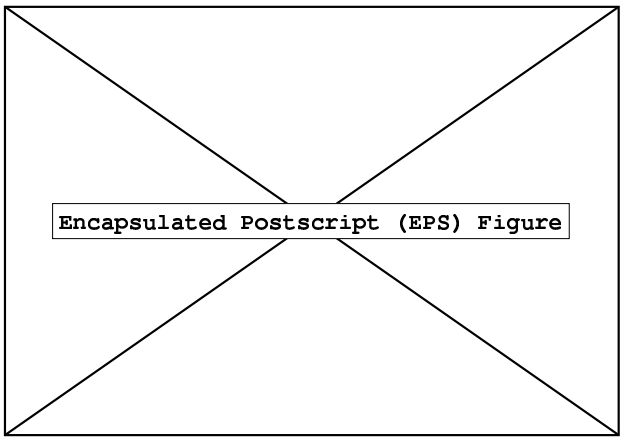

Fig. 1 Transition to landing for a VTVL vehicle.

Figure 1 presents a schematic of the last portion of a typical VTVL entry. The pitch-over maneuver, which occurs near Mach 0.2, is characterized by high angle of attack, unsteady, vortical flow. Accurately predicting vehicle performance during this aerodynamic pitch-over maneuver is quite challenging. While ground-based facilities can readily predict the vehicle's aerodynamics at discrete points during the maneuver, simulating the transient motion in a wind tunnel is difficult.[7] Time-dependent Computational Fluid Dynamics (CFD) offers another means of analyzing the pitch-over maneuver. The majority of work in unsteady CFD has, however, been restricted to small amplitude, harmonic variations in angle of attack in

*Research Engineer, Aerothermodynamics Branch, Aero- and Gas-Dynamics Division, Research and Technology Group.

†Deligent worker, AIAA member.

support of aeroelastic flutter predictions.[8]

The objective of the present work is to summarize the application of unsteady CFD methods to the problem of predicting VTVL vehicle aerodynamics during an un-powered pitch-over maneuver (further details are available in the companion conference paper[9]). In addition to the time-dependent simulation of a pitch-over maneuver, a series of steady solutions at discrete points are also computed for comparison with wind-tunnel measurements and as a means of quantifying unsteady effects. As this application represents a new challenge to unsteady CFD, observations concerning grid resolution, far-field boundary placement, temporal resolution, and the suitability of assuming flow-field symmetry are documented in Ref. 9.

Geometry

The vehicle's fore body is an 8 deg half-angle sphere cone with nose radius equal to 0.3 of the base radius. The aft body, beginning at the 85 percent fuselage station, is a cylinder with a partially squared-off cross-section producing flat "slices" extending from the base of the vehicle to approximately the 60 percent fuselage station. The vehicle has a fineness ratio of 6.4. A complete description of the vehicle geometry modeled has been given by Woods in Ref. 10.

Through the generosity of Karen Bibb, we have a demonstration of a subfigure situation. Note that with imbedded labels you can refer to Fig. 2 as a whole or specifically, things in Fig. 2(a) or Fig. 2(b). An early Lockheed-Martin X-33 configuration was used in the remainder of the examples. The full vehicle is shown in Fig. 2. This configuration (B1001A) was evaluated during Phase I of the X-33 program. It has twin vertical tails, fins, and outboard body flaps. The engines are modeled by the box-shaped structure on the base. *We can also have a "table" of two, or four, or more figures as in Fig. 3.*

Computational Mesh

The underlying surface definition database was generated from structured surface patches obtained using GRIDGEN,[11] GridTool,[12] and simple analytical methods. The unstructured surface and flow-field grids were then generated using FELISA[13] and TETMESH.[14] The coarsest mesh has 32,374 tetrahedra with 6,634 nodes. Additional meshes are described in Ref. 9; however, all the results shown here are the result of the coarsest meshes.

Since the flow about symmetric configurations at high angles of attack, even with zero side-slip, often involve asymmetric, vortex-dominated, features,[15–18] two different options for the computational domain were employed: one modeling the complete vehicle and another modeling only half of the vehicle, assuming symmetry across the pitch-plane. This aspect of the study is covered in Ref. 9.

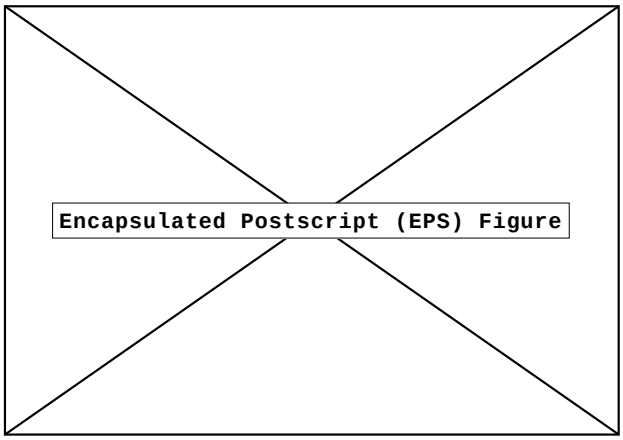

a) First pretty picture.

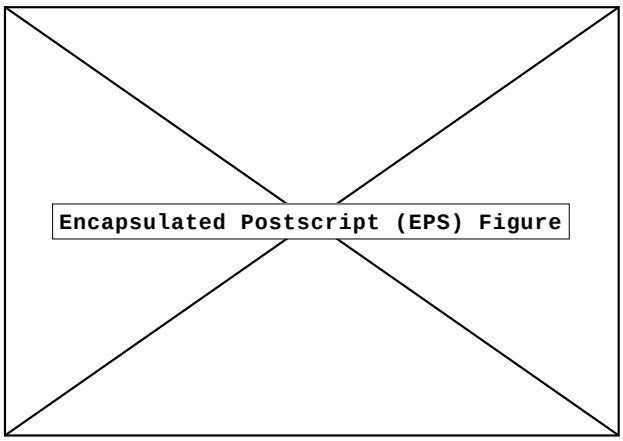

b) Second pretty picture.

Fig. 2 Temperature distribution comparisons at various wing semi-span stations as a function of chord. Whuh?

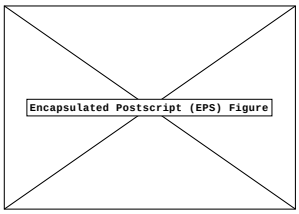

a) First pretty picture.

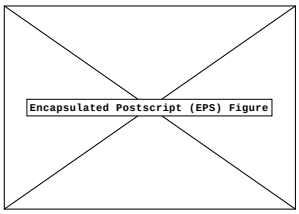

b) Second pretty picture.

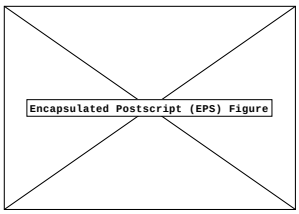

c) Second pretty picture, again.

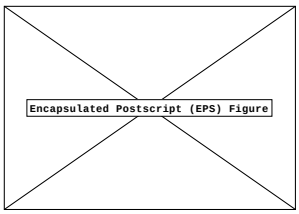

d) First pretty picture, again.

Fig. 3 Four small figures in a table-like setting.

Numerical Method

The 3D3U code of Batina[19] was used exclusively in this study. The 3D3U code was originally developed to study harmonically pitching wings and wing-bodies in transonic flow. The code can incorporate aeroelastic effects through assumed mode shapes, coupled with a deforming mesh via the linear spring analogy.

The following defaults were used for the computed results in this study: Roe's flux-difference splitting, an eigenvalue limiter threshold value of 0.3, second-order flux reconstruction using a κ of 0.5, and Gauss-Seidel implicit time integration with a CFL number of one million.

Maneuver Definition

The pitch schedule chosen for this study is the first half of a sine function. Initially, the vehicle is in steady flight at 17.5 degrees angle of attack, Mach 0.2. At time zero, the vehicle begins the pitch-over maneuver, reaching a maximum pitch rate exactly half-way through the maneuver and finishing at a 180 deg angle of attack. For this study, the time to complete the maneuver was chosen as 90 seconds, giving a maximum rotation rate of 3.1 deg per second halfway through the maneuver. For simplicity, it is assumed that the free-stream Mach number remains constant throughout the maneuver.

Sticking in a table for guidance (see Table 1). Normally there would be text following the table, so

Table 1 A sample table

Header 1		Header 2
a	b	c
d	e	f

that it is not left "hanging" into the next section.

Results

The main results are presented in two stages which are followed by comments on flow asymmetries for both steady and unsteady flows. The first stage is computed steady data as it compares to experimental results. while the second is a comparison of steady to unsteady data.

Steady Flow

As a baseline to examine the unsteady effects of the pitch-over maneuver itself, steady flow at selected angles of attack were computed. Figure 4 shows a comparison of the normal force coefficient with the experimental data of Woods[10] for angles of attack from 0 to 60 deg. The computed results agree well (within 20 percent) at small angles of attack, and diverge from the experimental results as the angle of attack increases largely due to the position of the lee-side separation line—a viscous phenomenon. Since the computed results are modeling inviscid flow, the only mechanism

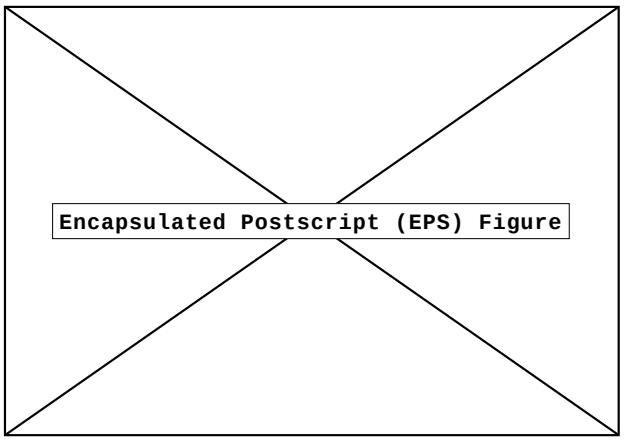

Fig. 4 Comparison of steady normal force coefficient as a function of angle of attack with experimental data of Woods[10]

for flow separation is the numerical dissipation in the scheme. Thus, the exact location of the computed separation line is highly grid and scheme dependent. Compounding this is the fact that the lee-side separation line nearly encompasses the length of the vehicle; and thus, a slight deviation can make a large difference in the integrated coefficients.

Unsteady Flow

Figure 5 compares the normal force coefficient of both the steady and unsteady calculations. The solid line represents the unsteady results and the symbols are the steady-flow results. Readily discernible is the fact that the steady and unsteady results are significantly different. The time-dependent results have the time lag behavior expected for moderately unsteady flow: showing the same general qualitative trend throughout the angle-of-attack range, but with the unsteady results lagging behind the steady results. Other aerodynamic coefficients show similar differences.[9]

Flow Asymmetry

As documented in Ref. 9, no appreciable asymmetries were found for the steady flow cases computed although they were present in the experimental data of Woods.[10] However, for the unsteady case, asymmetric flow is apparent as shown in Figuref:uasym. This figure shows the appearance of a non-zero side-force similar to that reported for *steady* flow by Woods.[10] The most significant manifestations of the asymmetries occur in the 90 to 135 deg angle-of-attack range.

Concluding Remarks

The objective of the present work was to focus an unsteady CFD method on the prediction of VTVL vehicle aerodynamics during a pitch-over maneuver. This was accomplished through the use of the inviscid 3D3U code[19] A series of steady solutions at discrete points in the maneuver were computed and it was

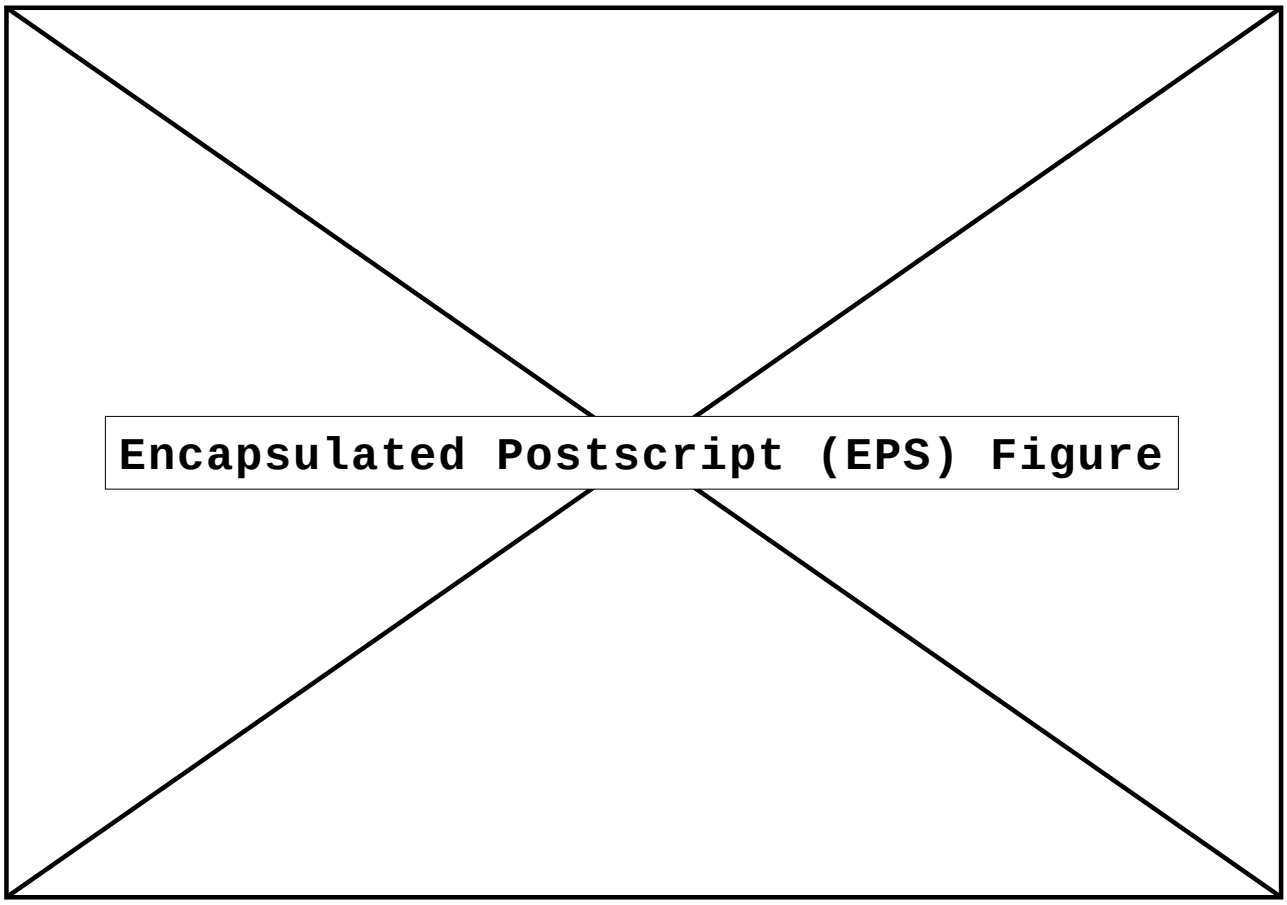

Fig. 5 Comparison of steady and unsteady normal force coefficients as a function of angle of attack. ***Example of a figure that spans both columns. The danger is that the figure numbering may be out of order since the single-column float and double-column float counters are not connected when it comes to determining placement order. You can correct this known "feature" of LaTeX by using the fix2col package.***

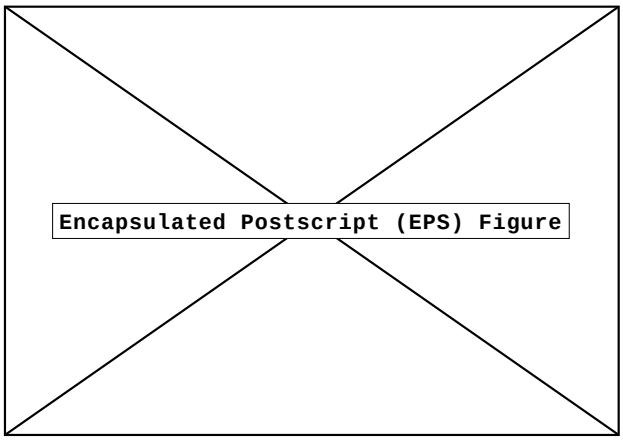

Fig. 6 Unsteady flow asymmetry: side force coefficient as a function of angle of attack.

shown that, even for the unrealistically slow pitch-over rate studied, unsteady effects were large. More importantly, the rotation maneuver creates flow asymmetries which lead to side forces not apparent for the steady cases.

As this is an exploratory study, there is certainly room for future work. The following is just a handful of extensions which would be necessary to create an effective design tool: incorporating viscous effects, allowing movable control surfaces, coupling a six-degree-of-freedom rigid body dynamics solver, adding control law, and incorporating an adaptive grid capability.

References

[1]Bekey, I., Powell, R., and Austin, R., "NASA Studies Access to Space," *Aerospace America*, May 1994, pp. 38–43.

[2]Dornheim, M. A., "NASA Awards RLV Contracts," *Aviation Week & Space Technology*, Jun. 1994, pp. 22–23.

[3]Austin, R. E. and Cook, S. A., "SSTO Rockets: Streamlining Access to Space," *Aerospace America*, Nov. 1994, pp. 34–38.

[4]Dornheim, M. A., "DC-X Demonstrates Key Maneuver," *Aviation Week & Space Technology*, Jul. 1995, pp. 56–59.

[5]David, L., "DC-X Completes Pivot Test Over White Sands," *Space News*, Vol. 6, No. 27, Jul. 1995, pp. 1,20.

[6]Dornheim, M. A., "DC-X Holds Promise; Big Questions Remain," *Aviation Week & Space Technology*, Aug. 1995, pp. 56–59.

[7]O'Leary, C. O., Weir, B., and Walker, J. M., "A New Rig for the Measurement of Rotary and Translational Derivatives," ICAS 94–3.4.1, Sep. 1994, In 19th Congress of the International Council of the Aeronautical Sciences ICAS Proceedings.

[8]Edwards, J. W. and Malone, J. B., "Current Status of Computational Methods for Transonic Unsteady Aerodynamics

and Aeroelastic Applications," *AGARD Conference Proceedings: Transonic Unsteady Aerodynamics and Aeroelasticity*, No. 507, Mar. 1992, pp. 1–1—1–24.

[9]Kleb, W. L., "Aerodynamic Characteristics of an Aerospace Vehicle During a Subsonic Pitch-Over Maneuver," AIAA Paper 96–0825, Jan. 1996.

[10]Woods, W. C. and Merski, N. R., "Aerodynamic Characteristics of a Vertical Takeoff / Vertical Landing (VTVL) Single Stage to Orbit Vehicle from M = 0.1 to 10," AIAA Paper 95–1828, 1995.

[11]Steinbrenner, J. P., Chawner, J. R., and Fouts, C. L., "The GRIDGEN 3D Multiple Block Grid Generation System," Wright Research and Development Center Report WRDC–TR–90–3022, Oct. 1989.

[12]Samareh-Abolhassani, J., "GridTool: A Surface Modeling and Grid Generation Tool," *Proceedings of the Workshop on Surface Modeling, Grid Generation, and Related Issues in CFD Solutions*, NASA CP–3291, May 1995, pp. 821–831.

[13]Peraire, J., Morgan, K., and Peiro, J., "Unstructured Finite Element Mesh Generation and Adaptive Procedures for CFD," *AGARD Conference Proceedings: Application of Mesh Generation to Complex 3-D Configurations*, No. 464, 1990, pp. 18.1–18.12.

[14]Kennon, S. R., Meyering, J. M., Berry, C. W., and Oden, J. T., "Geometry-Based Delaunay Tetrahedralization and Mesh Movement Strategies for Multi-Body CFD," AIAA Paper 92–4575, Aug. 1992.

[15]Yoshinaga, T., Tate, A., and Sekine, H., "Side Force of Blunted Circular Cylinders at High Angles of Attack in Supersonic Flow," AIAA Paper 94–3520, Aug. 1994, In AIAA Atmospheric Flight Mechanics Conference Proceedings.

[16]Cobleigh, B. R., "High-Angle-of-Attack Yawing Moment Asymmetry of the X-31 Aircraft from Flight Test," AIAA Paper 94–1803, Jun. 1994, In 12th AIAA Applied Aerodynamics Conference Proceedings.

[17]Dusing, D. W. and Orkwis, P. D., "On Computing Vortex Asymmetries About Cones at Angle of Attack Using the Conical Navier-Stokes Equations," AIAA Paper 93–3628, Aug. 1993, In AIAA Atmospheric Flight Mechanics Conference Proceedings.

[18]Fisher, D. F. and Cobleigh, B. R., "Controlling Forebody Asymmetries in Flight—Experience with Boundary Layer Transition Strips," AIAA Paper 94–1826, Jun. 1994, In 12th AIAA Applied Aerodynamics Conference Proceedings.

[19]Batina, J. T., "Implicit Upwind Solution Algorithms for Three-Dimensional Unstructured Meshes," *AIAA Journal*, Vol. 31, No. 5, May 1993, pp. 801–805, See also AIAA Paper 92–0447.